

Supporting Information:

Role of Additive Size in the Segmental Dynamics and Mechanical Properties of Cross-Linked Polymers

Xiangrui Zheng¹, Lan Xu², Jack F. Douglas^{3} and Wenjie Xia^{2*}*

¹Department of Mechanics, School of Aerospace Engineering,

Huazhong University of Science and Technology, Wuhan, 430074, China

²Department of Aerospace Engineering, Iowa State University, Ames, Iowa 50011, United States

³Materials Science and Engineering Division, National Institute of Standards and Technology,

Gaithersburg, Maryland 20899, United States

*Corresponding authors:

wxia@iastate.edu (Wenjie Xia)

jack.douglas@nist.gov (Jack F. Douglas)

Thermodynamical properties

Figure S1 (a-c) estimates the fundamental thermodynamical properties, including density ρ , reduced thermal expansion coefficient $\alpha_p^* = T\alpha_p$ and dimensionless isothermal compressibility $\kappa_T^* = \rho k_B T \kappa_T$ over a wide range of temperature T for cross-linked polymer/additive mixtures with a wide range of additive bead size. The introduction of additives leads to an increase in ρ and a reasonable decrease in α_p^* and κ_T^* . The difference in ρ between pure polymer and polymer/additive mixtures progressively increases with the bead size of additives decreasing, while the polymer/additive mixtures with smaller bead size exhibit a similar α_p^* and κ_T^* with pure polymer. In addition, compared to ρ and α_p^* , κ_T^* had a relatively weak dependence on the additive size.

The static structure factor $S_a(q)$ of additives in the polymer/additive mixtures at $T = 1.0 \text{ } \varepsilon / k_B$ is also shown in **Figure S1d**. The additive size has a remarkable influence on the structure of additives in terms of local density variations.¹ At small wavenumbers (q closes to 0), a tremendous increase is observed with the decreasing bead size, similar with the static structure factor curve of small particles observed in binary mixtures, which was related to phase separation.² With the wavenumber increasing ($q > 3$), the peak position at which $S_a(q)$ reaches its first peak varies non-monotonically with the additive size, where the mixtures with additive aggregation (system $\sigma_a = 0.3$) exhibited the smallest wavenumber at the first peak. Similarly, the time-resolved light scattering and X-ray scattering experiments both indicated that the peak scattering vector shifted to lower value and the scattering intensity increased continuously from the beginning of phase separation.³⁻

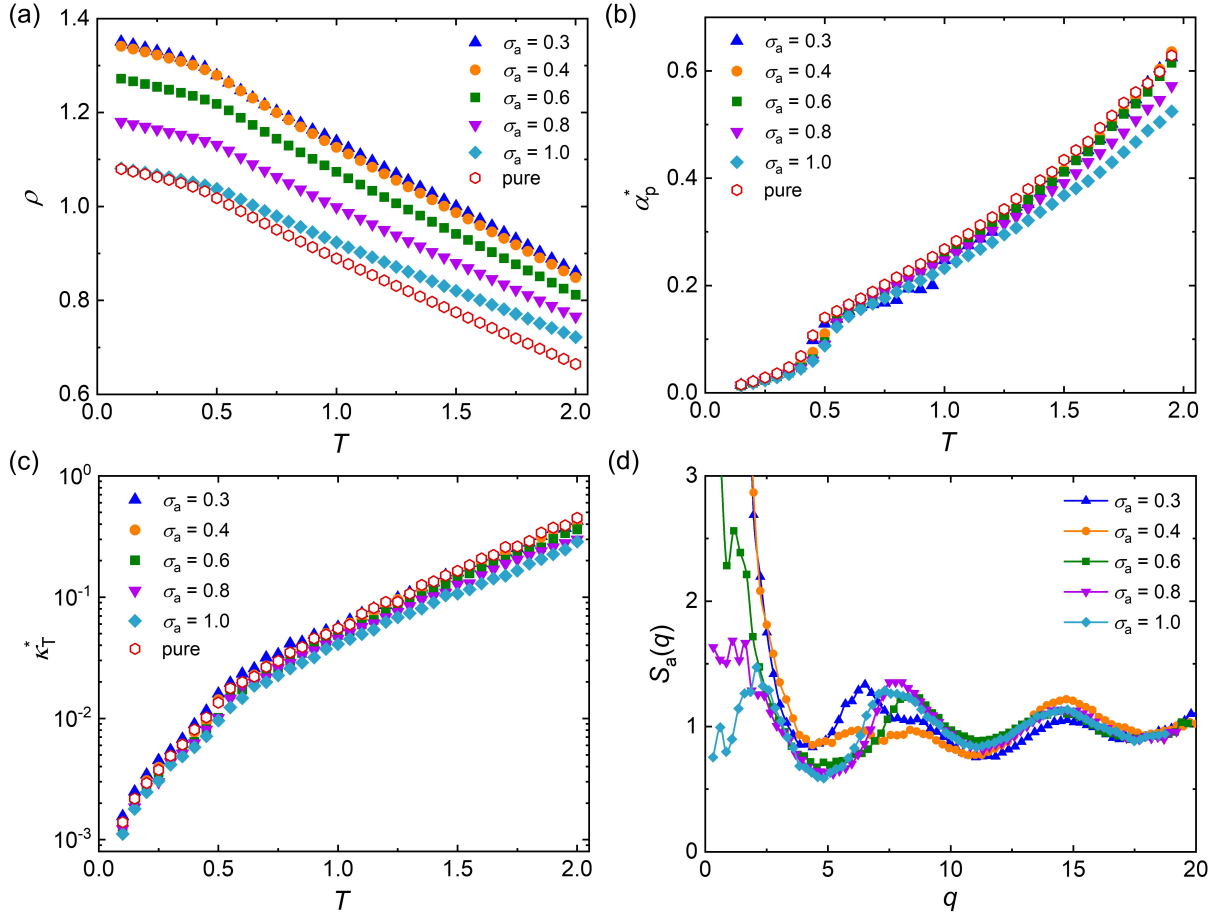


Figure S1. The thermodynamical properties for pure polymer and polymer/additive mixtures with varying additive size σ_a . (a) Number density ρ . (b) Reduced thermal expansion coefficient α_p^* . (c) Reduced isothermal compressibility κ_T^* . (d) Static structure factor $S_a(q)$ of the part of additives in polymer/additive mixtures at $T = 1.0 \epsilon/k_B$.

The effect of cross-link density

The additive aggregation phenomenon for cross-linked polymer/additive mixtures with lower cross-link density is estimated to investigate the mutual influences between cross-linking dynamics and aggregation of small additives. As shown in the **inset of Figure S2a**, the static structure factor of the whole mixture systems, $S_m(q)$, at the limit of q close to 0 decreases with the decrease of cross-link density, indicating a slightly weaker additive aggregation. In contrast, the $S_m(q)$ at larger q is independent of cross-link density, manifested by the collapsed curves at q larger than 2.5 (**Figure S2a**). The effects of cross-link density on the relaxation time and shear modulus for cross-

linked polymer/mixtures with variable additive size were also shown in **Figure S2b and S2c**. Increasing the cross-link density of cross-linked polymer leads to an increase in the relaxation time and shear modulus, consistent well with that observed in pure cross-linked polymers^{6,7} and cross-linked polymer/additive mixtures.⁸ In addition, the relaxation time and shear modulus both exhibit non-monotonic trends with the additive size for cross-linked polymers with variable cross-link density.

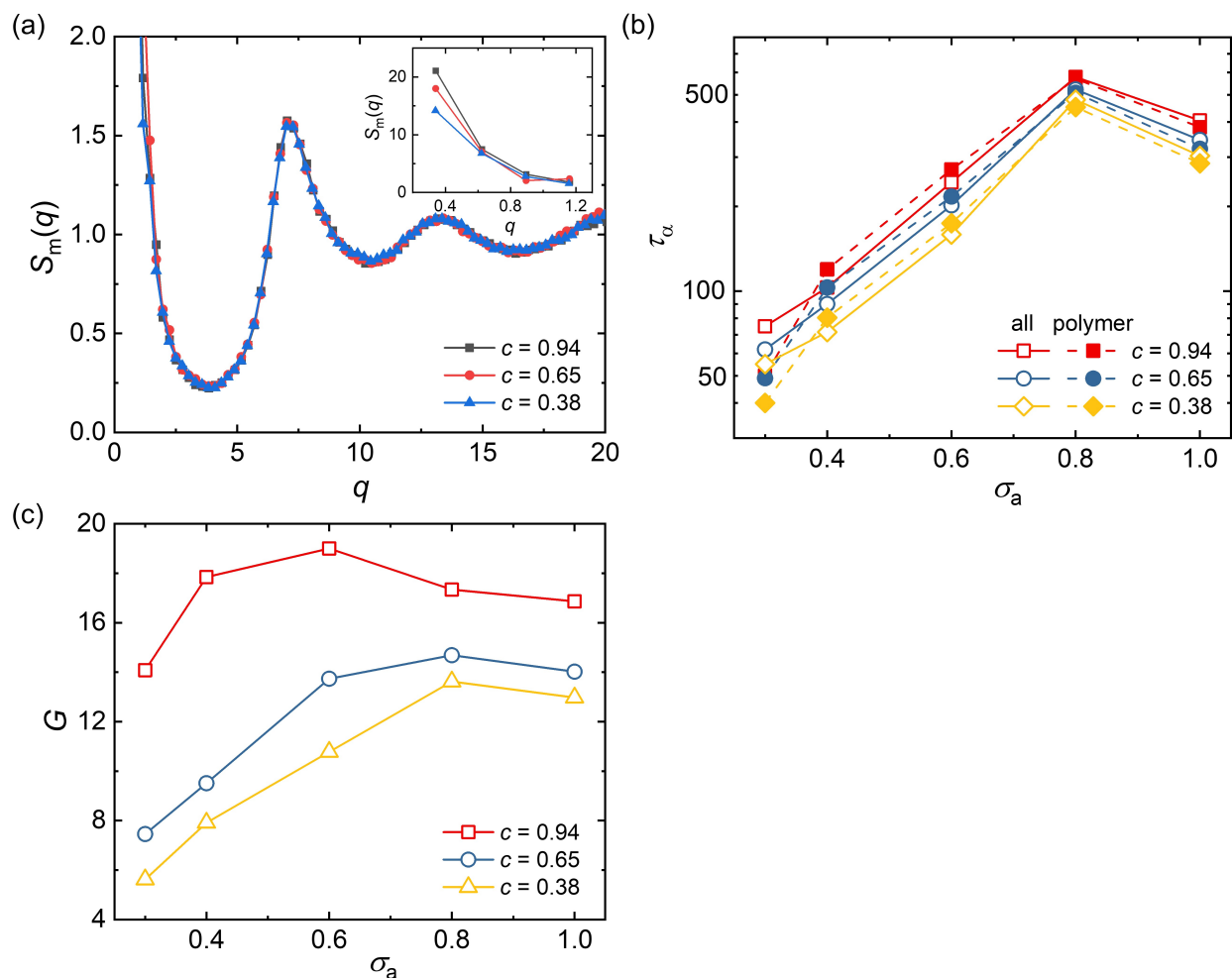


Figure S2. The effect of cross-link density. (a) The static structure factor $S_m(q)$ of polymer/additive mixtures with additive bead size $\sigma_a = 0.3 \sigma$ at $T = 1.0 \varepsilon / k_B$ for cross-linked polymer with varying variable cross-link density, c . The inset describes the $S_m(q)$ at the limit of q close to 0. (b) The structural relaxation time τ_α as a function of additive bead size σ_a for polymer/additive mixtures (open symbols) and partial τ_α of polymer (solid symbols) in polymer/additive mixtures. (c) The shear modulus G as a function of σ_a for polymer/additive mixtures.

The definition of Debye-Waller factor $\langle u^2 \rangle$

For the glass-forming polymer materials, Debye-Waller factor $\langle u^2 \rangle$ measures the rattling amplitude in the cage regime at the picosecond time scale,⁹⁻¹¹ which corresponds to the plateau in the mean-square displacement (MSD) versus time curves.¹² The mean-square displacement (MSD) of atoms is calculated according to the time evolution of atom coordinates,

$$\langle r^2(t) \rangle = \frac{1}{N} \left\langle \sum_{j=1}^N |\mathbf{r}_j(t) - \mathbf{r}_j(0)|^2 \right\rangle \quad (\text{S.1})$$

where \mathbf{r}_j is the position of monomer j , N is the total number of atoms in the system, and angled bracket indicates an ensemble average. **Figure S3** shows the MSD curves at $T = 0.5 \varepsilon / k_B$ for cross-linked polymer/additive mixtures with variable additive size. At short time, the MSD curve exhibits a profound increase with time corresponding to ballistic motion. With time increasing, the increasing trend of MSD curves gets slower and MSD curves gradually reach a plateau marking the cage regime. Based on the MSD curves, Debye-Waller factor $\langle u^2 \rangle$ is defined as MSD at $t = 1 \tau_{LJ}$ for cross-linked polymer/additive mixtures and pure polymer melt.

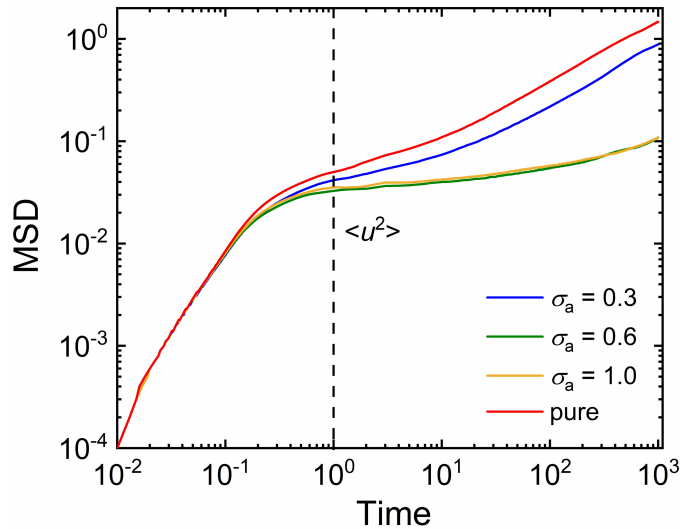


Figure S3. The MSD versus time curves for cross-linked polymer/additive mixtures with variable additive bead size and pure cross-linked polymer at $T = 0.5 \varepsilon / k_B$.

The polymer-additive interfacial interaction

The interfacial interaction between additives and cross-linked polymer is summarized in **Figure S4**. With additive segmental size decreasing, the additive-polymer interaction strength decreases progressively. When the additive size decreased to 0.3σ , the additive-polymer interaction strength is too weak and leads to occurrence of additive aggregation. And thus, the additive mobility (i.e., Debye-Waller factor) and shear modulus decreased significantly for mixtures with additive aggregation.

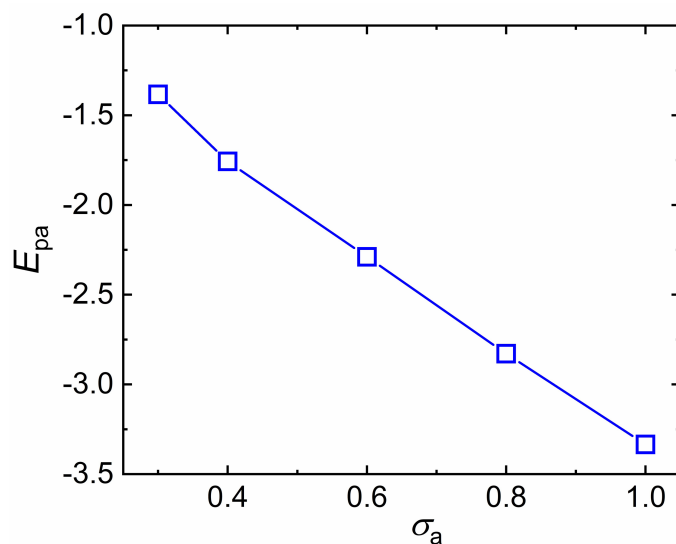


Figure S4. The interaction strength between cross-linked polymer and additives as a function of additive size.

The determination of bulk modulus

Figure S5a shows the bulk modulus B over a wide range of temperature T for polymer/additive mixtures with varying additive bead size, which is estimated from the reciprocal of isothermal compressibility of mixtures. The addition of additives with a wide range of bead size could improve the bulk modulus obviously. And the bulk modulus is dependent weakly on the additive bead size when the bead size of additives is larger than 0.4σ , while it exhibits a sudden decrease when the additive aggregation occurred. The overall variation trend in bulk modulus shows great agreement with that observed in shear modulus. Similarly, numerous experiments

have demonstrated that the phase separation would reduce the modulus and strength with various degrees of epoxy/additive blends.^{13–16}

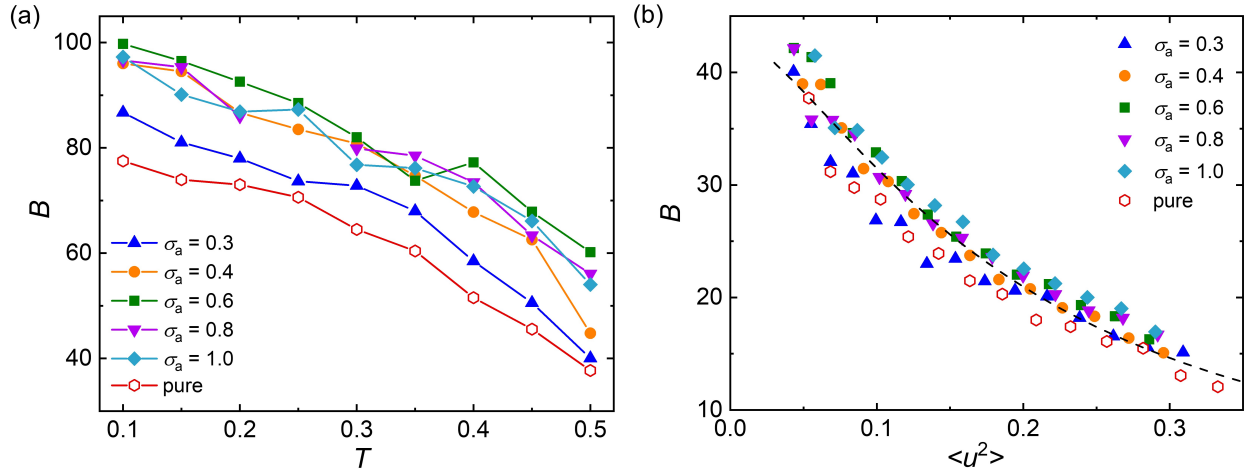


Figure S5. (a) The bulk moduli B as a function of temperature T for polymer/additive mixtures with varying additives size σ_a . (b) B as a function of Debye-Waller factor $\langle u^2 \rangle$. The dashed lines indicate the fitting results above glass transition temperature T_g with the function form $B = 1/[\kappa_T^0 \times (\langle u^2 \rangle / \langle u_A^2 \rangle)^{3/2} + \kappa_T^1]$, where $(\kappa_T^0 / \langle u_A^2 \rangle^{3/2}, \kappa_T^1)$ are fitting parameters. The fitting parameters $(\kappa_T^0 / \langle u_A^2 \rangle^{3/2}, \kappa_T^1)$ are (0.276, 0.023), and the coefficient of determination R^2 of fitting curves is 0.945.

Figure S5b further examines the scaling law between bulk moduli B and Debye-Waller factor $\langle u^2 \rangle$ for polymer/additive mixtures with varying additive bead size. An empirical function proposed by Douglas and Xu¹⁷ for the scaling relationship between isothermal compressibility and Debye-Waller factor, $\kappa_T - \kappa_T^1 = \kappa_T^0 \times (\langle u^2 \rangle / u_A^2)^{3/2}$, was used here, which has successfully described the scaling relationship for linear polymer melts with variable chain stiffness and pressure. The fitting curves (dashed line) is shown in **Figure S5b**, which demonstrates that the empirical function could describe the scaling relationship between B and $\langle u^2 \rangle$ reasonably for pure polymer and its mixtures with a wide range of additive size, as observed in pure cross-linked polymers with varying cross-link density, cohesive interaction strength and chain stiffness.^{6,7,18} It is notable that the

additive aggregation would not affect the scaling law between bulk modulus and Debye-Waller factor, consistent with that observed in the shear modulus. Most recently, this type of scaling expression was also confirmed in an atomistic model of polyethylene and functionalized polyethylene with varying number of functional groups.¹⁹

References

- 1 E. M. Zirdehi and F. Varnik, *J. Chem. Phys.*, 2019, **150**, 024903.
- 2 V. Vaibhav, J. Horbach and P. Chaudhuri, *J. Chem. Phys.*, 2022, **156**, 244501.
- 3 G. Shen, Z. Hu, Z. Liu, R. Wen, X. Tang and Y. Yu, *RSC Adv.*, 2016, **6**, 34120–34130.
- 4 Z. Xia, W. Li, J. Ding, A. Li and W. Gan, *J. Polym. Sci. Part B Polym. Phys.*, 2014, **52**, 1395–1402.
- 5 G. Li, Z. Huang, C. Xin, P. Li, X. Jia, B. Wang, Y. He, S. Ryu and X. Yang, *Mater. Chem. Phys.*, 2009, **118**, 398–404.
- 6 X. Zheng, Y. Guo, J. F. Douglas and W. Xia, *J. Chem. Phys.*, 2022, **157**, 064901.
- 7 X. Zheng, Y. Guo, J. F. Douglas and W. Xia, *Macromolecules*, 2022, **55**, 9990–10004.
- 8 W. Nie, Y. Liao, S. Ghazanfari, Y. Wang, X. Wang, Y. Huang and W. Xia, *Polym. Compos.*, 2024, **45**, 8508–8526.
- 9 Y. Wang, Z. Li, K. Niu, W. Xia and A. Giuntoli, *Macromolecules*, 2024, **57**, 5130–5142.
- 10 A. Alesadi and W. Xia, *Macromolecules*, 2020, **53**, 2754–2763.
- 11 X. Wang, H. Zhang and J. F. Douglas, *J. Chem. Phys.*, 2021, **155**, 204504.
- 12 J. Li, B. Zhang and Y. Li, *Macromolecules*, 2023, **56**, 589–600.
- 13 V. S. Mathew, C. Sinturel, S. C. George and S. Thomas, *J. Mater. Sci.*, 2010, **45**, 1769–1781.
- 14 Y. Liu, W. Zhang and H. Zhou, *Polym. Int.*, 2005, **54**, 1408–1415.
- 15 Z. Sun, L. Xu, Z. Chen, Y. Wang, R. Tusiime, C. Cheng, S. Zhou, Y. Liu, M. Yu and H. Zhang, *Polymers*, 2019, **11**, 461.
- 16 L. Dong, W. Zhou, X. Sui, Z. Wang, H. Cai, P. Wu, J. Zuo and X. Liu, *J. Electron. Mater.*, 2016, **45**, 3776–3785.
- 17 J. F. Douglas and W.-S. Xu, *Macromolecules*, 2021, **54**, 3247–3269.
- 18 X. Zheng, W. Nie, Y. Guo, J. F. Douglas and W. Xia, *Macromolecules*, 2023, **56**, 7636–7650.
- 19 C. Jeong, F. W. Starr, K. L. Beers and J. F. Douglas, *Macromolecules*, 2023, **56**, 3873–3883.